



Effects of global ship emissions on European air pollution levels

Jan Eiof Jonson¹, Michael Gauss¹, Michael Schulz¹, Jukka-Pekka Jalkanen², and Hilde Fagerli¹

¹Norwegian Meteorological Institute, Oslo, Norway

²Finnish Meteorological Institute, Helsinki, Finland

Correspondence to: Jan Eiof Jonson (j.e.jonson@met.no)

Abstract.

Ship emissions constitute a large, and so far poorly regulated, source of air pollution. Emissions are mainly clustered along major ship routes, both in open seas and close to densely populated shorelines. Major air pollutants emitted include sulfur dioxide, NO_x and particles. Sulfur dioxide and NO_x are both major contributors to the formation of secondary fine particles (PM_{2.5}) and to acidification and eutrophication. In addition, NO_x is a major precursor for ground-level ozone.

This study is based on global and regional model calculations. The model runs are made with meteorology and emission data representative for year 2017, after the tightening of the SECA (Sulphur Emission Control Area) regulations in 2015, but before the global sulfur cap entering into force in 2020. We have also made model runs reducing sulfur emissions by 80% corresponding to the 2020 requirements. This study is based on model sensitivity studies perturbing emissions from different sea areas: the Northern European SECA in the North Sea and the Baltic Sea, the Mediterranean Sea and the Black Sea, the Atlantic Ocean close to Europe, shipping in the rest of the world and finally all global ship emissions together. Sensitivity studies have also been made setting lower bounds on the effects of ship plumes on ozone formation.

The results from the global and regional calculations are similar. Both global and regional scale calculations show that for PM_{2.5} and depositions of oxidised nitrogen and sulfur, the effects of ship emissions are much larger when emissions occur close to the shore than at open seas. In many coastal countries calculations show that shipping is responsible for 10% or more of the controllable PM_{2.5} concentrations and depositions of oxidised nitrogen and sulphur. For ozone the lifetime in the atmosphere is much longer than for PM_{2.5}, and the potential for ozone formation is much larger in otherwise pristine environments. We find considerable contributions from open sea shipping. As a



result the largest contributions to ozone in several regions and countries are from rest of the world shipping.

25 1 Introduction

As shown by both model calculations and measurements, concentrations of almost all air pollutants have decreased throughout most of Europe since 1990 Colette et al. (2016, 2017). Over the same time span, depositions of eutrophying and in particular acidifying species have also decreased (Theobald et al., 2019). These trends are, with the partial exception of ground level ozone, almost entirely driven
30 by reductions in European emissions (Colette et al., 2016). Since year 2000, European emission trends are diverse, with general downward trends in Western European countries and an upward trends in Eastern Europe (Gaisbauer et al., 2019). The latter upward trend is largely driven by an economic recovery in former Soviet Union states.

Emissions from international shipping to air, relevant in the context of air pollution and depositions
35 in Europe, include particulate matter, oxides of sulphur and nitrogen, CO and NMVOC (Non-Methane Volatile Organic Carbon). Trends in emissions from shipping are less certain than for land based emissions, and differ depending on species and sea area. In general emissions from shipping have changed less than land based emissions in Western Europe (Gaisbauer et al., 2019), and, as a result, the relative contribution of ship emissions to air pollution in western parts of Europe has increased.
40 One notable exception is the SECA (Sulphur Emission Control Area) regions in the Baltic Sea and the North Sea, where sulfur emissions have dropped by more than an order of magnitude in the last decade. In the SECAs the maximum allowed sulphur content in fuels, and consequently the emissions from shipping, has been reduced in several steps with the latest, and most significant, measure implemented from January 2015 reducing the maximum allowed sulfur content in marine fuels from 1% to 0.1%.
45 Fuels with higher sulphur content may be used in combination with technology reducing sulphur emission to levels equivalent to the use of low-sulfur fuels. In addition the EU sulphur directive requires ships to use fuel with 0.1 % sulfur in EU harbour areas. From 2020 a global cap on sulfur content in marine fuels of 0.5% has been implemented as opposed to an average of about 2.5 % prior to 2020.

50 The global effects of international shipping on air pollution and depositions have already been identified in several papers (Corbett et al., 2007; Endresen et al., 2003; Eyring et al., 2007; Sofiev et al., 2018). In a global model calculation, Jonson et al. (2018a) found that a large portion of the anthropogenic contributions to $PM_{2.5}$ and depositions of sulphur and nitrogen in European coastal regions can be attributed to ship emissions in nearby sea areas. For boundary layer ozone the same
55 study showed a mixed result, with overall percentage contributions to ozone of antropogenic origin of more than 20% in several Mediterranean countries, and negative contributions in some countries bordering the North Sea caused by ozone titration. In Jonson et al. (2018b) the effects of pollution



from other continents, including also the effects of international shipping on European air pollution were investigated within the framework of TF_HTAP2 (Task Force on Hemispheric Transport of Air Pollution, phase II). These calculations indicated that more than 10% of the ozone in Europe of anthropogenic origin can be attributed to international shipping. The percentage contributions were similar for both annually averaged ozone and for ozone indicators such as SOMO35¹ and POD₁ (deciduous) forest².

In this paper we study the effects of global international shipping further by performing a series of model scenario calculations perturbing ship emissions, both globally and from individual sea areas, to attribute the effects of ship emissions on European countries from different sea areas. We have limited the study to air concentrations of PM_{2.5} and ozone, and to depositions of oxidised nitrogen and sulfur. The calculations are made with meteorology and emissions for year 2017, but calculations are also made for 2020 and beyond, by scaling sulfur emissions outside the North Sea and Baltic Sea SECAs by 0.5/2.5 (a decrease in the sulfur content in marine fuels from about 2.5% to 0.5%), reflecting the expected reductions in sulfur emissions following the CAP2020 regulations implemented in 2020, see <http://www.imo.org/en/mediacentre/hottopics/pages/sulphur-2020.aspx>.

The global model calculations are compared to the regional scale source receptor calculations, also for year 2017, included in the latest EMEP report (EMEP Status Report 1/2019, 2019).

Finally, sensitivity tests have been made to give bounds for the effect of chemistry within exhaust plumes: In pristine environments, pollutant concentrations can be orders of magnitude higher within ship plumes than in their surroundings, whereas in the model these emissions plumes are instantly diluted into a large grid volume. Ignoring the chemistry within the plumes can potentially result in an overestimation of ozone.

2 Model description

Concentrations of air pollutants and depositions of sulphur and nitrogen have been calculated with the EMEP MSC-W model version rv4.34 (hereafter 'EMEP model') on a global model domain with a 0.5° x 0.5° longitude-latitude resolution. The EMEP model is a comprehensive air quality model which has been used extensively during the last four decades for air pollution research and to underpin international air quality legislation. It takes into account processes of emissions, advection, turbulent diffusion, chemical transformations, wet and dry depositions. The calculations of dry depositions are made separately for each sub-grid land-cover classification. These sub-grid estimates are aggregated

¹SOMO35 (Sum of Ozone Means Over 35 ppb) is the indicator for health impact assessment recommended by WHO. It is defined as the yearly sum of the daily maximum of the running 8-hour running average of ozone above 35 ppb.

²POD₁ (Phyto-toxic Ozone Dose for deciduous forests) is the accumulated stomatal ozone flux over a threshold Y integrated from the start to the end of the growing season. For deciduous forests, the critical level of 4 mmol m⁻² is exceeded in most of Europe, indicating a risk of ozone damage to forests. See Mills et al. (2011a, b) for further description of this metric.



to provide output deposition estimates for broader ecosystem categories as deciduous and coniferous forests.

90 For comparison we also include results from the regional model calculations included in the latest EMEP report (EMEP Status Report 1/2019, 2019) covering the geographical area between 30°N–82° and 30°W–90°E on a 0.3° x 0.2° longitude-latitude resolution. Both the global and regional regional calculations have been made using 2017 meteorological input data and 2017 emissions. The meteorological input data are from the European Centre for Medium-Range Weather Forecasts
95 (ECMWF) based on the CY40R1 version of their IFS (Integrated Forecast System) model.

A detailed description of the EMEP model can be found in Simpson et al. (2012) with later model updates being described in Simpson et al. (2019) and references therein. The EMEP model is available as Open Source (see <https://github.com/metno/emep-ctm>). The EMEP model is under continuous development, and undergoes extensive evaluation against measurements every year as part of the
100 EMEP status reports, see Gauss et al. (2017, 2018, 2019) for evaluations of the latest emission years available, 2015, 2016 and 2017. The model is also evaluated daily and openly within the Copernicus Atmosphere Monitoring Service, where it is used operationally for regional air quality forecasts and analyses (see <https://www.regional.atmosphere.copernicus.eu/>). In addition, the EMEP regional model has successfully participated in model inter-comparisons and model evaluations in a number of
105 peer-reviewed publications (Colette et al., 2011, 2012; Angelbratt et al., 2011; Dore et al., 2015; Karl et al., 2019). In Vivanco et al. (2018), depositions of sulfur and nitrogen species in Europe calculated by 14 regional models were evaluated against measurements showing good results for the EMEP model. In global mode the model has also participated in a number of model inter-comparisons and model evaluations (Stjern et al., 2016; Tan et al., 2018; Liang et al., 2018; Jonson et al., 2018a). At
110 least for background sites, the performance is comparable for regional and global model applications.

2.1 Emissions

For the global calculations land-based emissions have been provided by the International Institute for Applied Systems Analysis (IIASA) within the European FP7 project ECLIPSE (<http://www.iiasa.ac.at/web/home/research/researchPrograms/air/ECLIPSEv5.html>). In this study we use ECLIPSE
115 version 6a (hereafter referred to as 'ECLIPSEv6a'), which is a global emission data set on 0.5 x 0.5 degree resolution and is widely used by the scientific community. Some of the methods used in ECLIPSE are described in the recent publication of Höglund-Isaksson et al. (2020). Historical data rely on statistical data (until 2015) for energy from the International Energy Agency (IEA), agricultural data from the United Nations Food and Agriculture Organisation (FAO), the International
120 Fertiliser Association (IFA), and additional data for mineral industries from United States Geological Survey (USGS), and numerous additional sources for informal industries (e.g., brick making), waste, etc. Current baseline projections rely on the New Policies Scenario (NPS) from the World Energy Outlook 2018 of IEA (IEA, 2018) FAO projections, and for EU agriculture also on the European-wide



farmtype model in CAPRI (Common Agricultural Policy Regional Impact). ECLIPSEv6a emissions
125 are available in 5-year intervals from 2005 onward. In this study the emissions are interpolated to
2017.

The land-based emissions used in the regional model calculations are described in Gaisbauer
et al. (2019) and are mainly based on the officially reported data from the countries. In Table 1
these officially reported emissions are listed aggregated for the EU27 countries compared to the
130 ECLIPSEv6a emissions. Differences are of similar magnitude for the individual EU countries. The
most significant difference is for sulfur, where the ECLIPSEv6a emissions are of the order of 15%
higher than those reported to EMEP.

Ship emission data sets used in both the global and regional model calculations are originally from
the Finnish Meteorological Institute, based on AIS data processed in the STEAM model (Johansson
et al., 2017) and downloaded from the ECCAD database (<https://eccad.aeris-data.fr/>). Ship emissions
135 of various species, based on the global data set, are listed in Table 1 separately for the Baltic Sea, the
North Sea (including the English Channel), the Mediterranean Sea and the Black Sea. In addition
emissions are listed for the remaining Atlantic area outside Europe, but bounded by 30 – 82 degrees
north and 30 degrees west to 90 degrees east corresponding to the "Northeast Atlantic Ocean"
140 also included in the regional calculations. These three sea areas are depicted in Figure 1. Finally
emissions are also listed for the total global sea area. Annual ship emissions used in the regional
model calculations are based on the same source (Gaisbauer et al., 2019). Even so, ship emissions
used in the global calculations are somewhat higher than in the regional calculations (see EMEP
Status Report 1/2019 (2019), appendix B).

145 In the FMI emission data all PM emissions are assumed to be emitted as PM_{2.5}. Emissions from
leisure boats are not included. In a separate study Johansson et al. (2020) have quantified the emissions
from leisure boats in the Baltic Sea only. Compared to emissions from the commercial fleet these
emissions were insignificant for NO_x and PMs. However, in regard to emissions of NMVOC the
study concluded that these can be significantly larger from leisure boats than from registered vessels
150 in the Baltic Sea, especially during summer (about 500% larger). However, as shown in Table 1,
land-based NMVOC and NO_x emissions are of similar magnitude, the NMVOX to NO_x ratio is very
small for ship emissions.

2.2 Definition of the model sensitivity tests

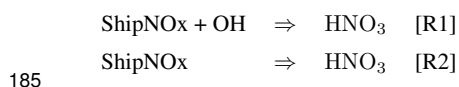
In order to calculate the effects of ship emissions on air pollution and depositions in Europe we
155 use a similar approach as in the SR (Source Receptor) calculations within the EMEP programme
(see EMEP Status Report 1/2019 (2019) appendix C as the latest example) reducing emissions by
15% from the individual countries/sea areas. The global model runs are made for a full calendar
year (2017) with a 5 month spin-up for several of the model runs as some of the species have a long
lifetime in the atmosphere (one month of more). Whereas in the EMEP SR calculations emissions



160 of different species are reduced in separate perturbation runs, we here reduce the emissions of all
species simultaneously in the same perturbation run, reducing the number of model runs to one for
each of the model scenarios listed in Table 2. We have combined the North Sea and the Baltic Sea
into one scenario run because they are both designated as SECA areas. Likewise we have combined
the Mediterranean Sea and the Black Sea. The sea areas are shown in Figure 1. ROW (Rest Of World)
165 are all sea areas not included in the sea areas listed above. We have also made additional model runs
with sulfur emissions from ships reduced to CAP2020 levels.

In the interpretation of the model results below we let the difference between the Base_2017 and
the SR_AllAnt model runs (see Table 2) represent 100% of the effects of all anthropogenic, and thus
controllable, global emissions. Similarly we calculate the contributions from global shipping as a
170 whole, or from shipping in a specific area, by subtracting the scenario run for shipping as a whole
or from a specific sea area from the Base model run. In this way we can relate the effects of ship
emissions in different regions to the total anthropogenic contribution. Even though not strictly linear,
this is a widely used approach that was also taken in the TF_HTAP phase II modelling exercise (see
workplan under <http://www.htap.org/>). For all depositions and air concentrations except ozone (and
175 ozone metrics) we add up the SR runs for the individual sea areas (SR_BALNOS, SR_MEDBLS,
SR_ATL and SR_ROW) and compare with the SR_AllSh emission perturbation providing a measure
of the linearity in the calculations.

In the model calculations described above, the ship emissions are instantly diluted throughout the
model grid cells in which the emissions occur. Previous studies (Vinken et al., 2011; Huszar et al.,
180 2010) have shown that this can lead to an overestimation of ozone formation, in particular in sea
areas where NO_x concentrations are otherwise low. The EMEP model has an option for splitting 50%
of the NO_x emissions from shipping into a pseudo-species "ShipNOx", see Simpson et al. (2015).
ShipNOx deposits as NO₂, but undergoes simple atmospheric reactions:



Reaction R1 proceeds with the same rate as the normal NO₂ + OH reaction, thus proceeding faster in
daylight and in high OH areas. Reaction R2 provides a minimum half-life of about 6 hours, loosely
based upon results shown in Vinken et al. (2011). We have repeated the calculations for the scenarios
listed above with the ShipNOx reactions included. We then assume that the calculations with and
190 without the ShipNOx split represent a lower and an upper limit of the effects of NO_x emissions from
shipping on the formation of ozone both globally and in the individual sea areas.

3 Model results

In this section we show the calculated effects of all global ship emissions, and the effects of emissions
from separate sea areas as defined in the separate scenarios in Section 2.2 . For ozone we also include



195 a discussion on the effects of the ShipNOx split and for PM_{2.5} we include the effects of the CAP2020 regulations.

3.1 PM_{2.5}

Figure 2 shows the global concentration of PM_{2.5} (a) and the contributions from global shipping (b). Globally the highest concentrations are calculated over parts of Asia and North Africa. In Europe
200 high concentrations are calculated in several locations with the highest concentrations in the Po Valley in Italy. The largest contributions from shipping are mainly calculated in and around the major ship tracks. In Figure 3 we show to what extent ship emissions from different sea areas contribute to the European PM_{2.5} concentrations seasonally. From all sea areas the largest effects are calculated in nearby countries/regions. Ship emissions generally peak in summer, but the seasonal variations in
205 emissions are not large, and far from large enough to explain the seasonal variations in concentrations seen in Figure 3. The main sources for particles and particle formation from shipping are NO₂ and sulfur (of which more than 95% is emitted as SO₂ in the gas phase, and the rest as sulphate particles). In addition ash, EC (Elemental Carbon) and OC (Organic Carbon) are assumed emitted as primary particles. The main oxidation paths for SO₂ are the OH reaction in the gas phase and in-cloud
210 oxidation (mainly with H₂O₂). Both these oxidants have a clear summer maximum, contributing to a summer maximum also for sulphate. In sea areas outside the SECAs sulphate makes up 50 to 80% of the PM_{2.5}, dry mass (Figure 8a), explaining the summer maximum in PM_{2.5} concentrations in most sea areas.

NO₂ is oxidised to gaseous HNO₃. HNO₃ can then react with sea salt forming particulate sodium
215 nitrate. However, in the presence of ammonia the formation of ammonium nitrate particles can be a lot faster. The latter reaction requires a surplus of NH₃ over sulfate. Ammonia is mainly emitted from agriculture with a seasonal maximum in spring. In the SECAs, where sulfur emissions from ships are very low, we calculate that nitrates make up almost 50% of the PM_{2.5} dry mass.

In addition both sulfate and nitrate from shipping results in an increase in ammonium (ammonium
220 nitrate and ammonium sulfate). About 20 to 30% of the PM_{2.5} mass over Europe is ammonium.

The effects of the emissions from individual sea areas on PM_{2.5} discussed below are based on 2017 ship emissions. The effects of the CAP2020 global reductions in sulfur emissions from ships are described in Section 4.

3.1.1 Contributions from the North Sea and the Baltic Sea

225 For countries/regions bordering the North Sea and the Baltic Sea (Figure 3 a,b,c,d) PM_{2.5} from local shipping peaks in spring. Following the implementation of the stricter SECA regulations from 2015, sulfur emissions are low (see Table 1). In particular the southwestern parts of this sea area are close to some of the highest ammonia emission regions in Europe. The main source of particles from shipping is NO₂ through the formation of nitrate, predominantly ammonium nitrate. The spring maximum in



230 $PM_{2.5}$ from the North Sea and the Baltic Sea shipping is caused by the interaction with ammonia
emissions, mainly from agriculture, peaking in spring.

3.1.2 Contributions from the Northeast Atlantic Ocean

The largest contributions to $PM_{2.5}$ concentrations in Europe from shipping in the Northeast Atlantic
(see Figure 3 e,f,g,h) are calculated for the regions bordering the ship track in and out of the
235 Mediterranean through Gibraltar, extending north to the English Channel. As this region is outside the
SECA, sulfur emissions are high, and a major constituent in $PM_{2.5}$ from shipping is sulfur, emitted
mainly as gaseous SO_2 and then oxidised to sulfate. The summer maximum in the contributions from
the Northeast Atlantic is mainly caused by sulfate.

3.1.3 Contributions from the Mediterranean Sea and the Black Sea

240 The largest contributions to $PM_{2.5}$ concentrations from shipping in the Mediterranean and Black
Sea region are calculated in and around the shipping lane from Gibraltar to the Suez Canal. High
concentrations are also calculated in and around the Adriatic Sea and around some of the major ports
like Marseille in France and Pireus in Greece. As in the NE Atlantic sulfur emissions from shipping
are high, and the summer maximum in this sea area is mainly caused by sulfate.

245 3.1.4 Contributions from Rest of world shipping

Given the large distance to the European continent, contributions to European $PM_{2.5}$ levels from
ROW shipping are small.

3.1.5 Country attributions

The source receptor relationships for shipping (total and from separate sea areas) are listed in Table 3
250 for selected countries. Here we also list the corresponding source receptor results as reported in the
latest EMEP report (EMEP Status Report 1/2019, 2019). In general, the reported relationships and
the results from the global model are in good agreement. Differences between the global and regional
calculations are discussed in Sections 5.

In Figure 4 the percentage contributions from all ships and from emissions in different sea areas to
255 selected European countries are shown. The contributions are calculated from the scenarios listed
in Section 2.2. We let the difference between the Base_2017 and the SR_All represent 100% of the
anthropogenic contributions to $PM_{2.5}$. The contributions from the individual sea areas are stacked on
top of each other and shown in parallel to the contributions from all ships (Base_2017 - SR_AllSh).
Any difference in the length of the two bars can be interpreted as a measure of non-linearities in the
260 calculations. Moderate deviations from linearity are in particular seen for the countries bordering
the southern parts of the North Sea caused by differences in ammonium nitrate formation between
the model scenarios. The contributions from all ships are split into a black and grey part where the



first grey part represents the contributions with CAP2020 sulfur emissions and the black part the additional contributions when using 2017 emissions, i.e. prior to the implementation of CAP2020.
265 The effects of the CAP2020 regulations are discussed in more detail in Section 4.

The figure clearly shows that the countries are most affected by nearby ship emissions, in particular in smaller countries close to major shipping lanes. Malta in the Mediterranean Sea, and Denmark bordering both the North Sea and the Baltic Sea, are the two countries most affected. Countries bordering only the Mediterranean Sea and the Black Sea are hardly impacted by other sea areas. A
270 few countries are bordering more than one of the separate sea areas. As an example Norway and UK are strongly impacted by both North Sea and remaining Atlantic ship emissions, Spain by the remaining Atlantic and the Mediterranean Sea. France is a "tricolore" country affected by the nearby North Sea, Mediterranean Sea and remaining Atlantic ship emissions.

3.2 Ozone

275 Figure 2c shows the global concentration of O₃ and Figure 2d the contributions from global shipping. Globally the highest concentrations are calculated for the latitudinal band between 20 to 40 degrees north. The largest contributions from shipping are mainly calculated in and around the major ship tracks in south Asia, resulting from high NO_x emissions in combination with favourable meteorological conditions for ozone production. In Europe there are similar favourable conditions in and
280 around the Mediterranean Sea. Below we discuss how ship emissions from different sea areas affect European ozone levels split by season.

Net formation of ozone depend on the ratio between NO_x and NMVOC. In regions with high NO_x concentration ozone production is limited by the availability of NMVOC, and further enhancements of NO_x will lead to increased ozone titration, and thus reductions of ozone, predominantly in the
285 winter months. In summer additional NMVOC emissions from leisure boats may lead to an increase in ozone levels in such areas. In areas limited by the availability of NO_x additional NO_x will result in increased ozone production, predominantly in the summer months.

3.2.1 North Sea and Baltic Sea

In the North Sea and Baltic Sea regions (Figure 5a,b,c,d), ship emissions contribute to widespread
290 ozone titration in all four seasons. The strongest titration effects are calculated in winter and the least in summer.

3.2.2 Northeast Atlantic

Although there is a net ozone loss throughout much of the year in the shipping lane from Gibraltar to the entrance of the English Channel, shipping contributes to higher ozone in most of the bordering
295 countries all year with the exception of the UK, northern Scandinavia and coastal regions next to the shipping lanes. Net ozone is in particular high in summer (Figure 5 e,f,g,h).



3.2.3 Mediterranean Sea and Black Sea

In the Mediterranean Sea and the Black Sea there is widespread ozone titration close to major shipping lanes and ports in winter (Figure 5i,j,k,l). However, in Spring ozone production starts to dominate, reaching a maximum in summer with contributions from shipping of more than 4ppb in the eastern Mediterranean sea and bordering land areas.

3.2.4 Rest of world shipping

Emissions from Rest Of World shipping affects all of Europe, but western and northern Europe more than southern and eastern Europe (Figure 5 m,n,o,p). The seasonal behaviour differs from the other sea areas with a summer minimum and a slight winter maximum. On an annual basis contributions are comparable, and in some regions higher, than contributions from the other sea areas.

3.2.5 Country attributions

For SOMO35³ the source receptor relationships for shipping (total and from separate sea areas) are listed in Table 4 for selected countries. We also list the corresponding source receptor calculations as reported in the latest EMEP report (EMEP Status Report 1/2019, 2019) and these results are discussed in Section 5.

In Figure 6a,c the contributions from all ship emissions and from emissions in different sea areas to selected European countries are shown for annually averaged ozone in ppb following 15% reductions in ship emissions in the sea areas. The calculated effects of 15% reductions in all anthropogenic emissions are given as numbers in the figure. In Figure 6b,d the effects of ship emissions on SOMO35 are given as a percentage of the total anthropogenic contributions. Given the non-linear behaviour of the ozone chemistry, contributions from the separate sea areas are not stacked (as for PM_{2.5} in Figure 3). The full length of the bars are split so that the first, darker part, of the bars represent the calculations with the ShipNOX parameterisation included as described in Section 2.2 and the second, brighter coloured part, the calculations without ShipNOX. The difference between the calculations with and without ShipNOX can be interpreted as a range for the effects of ship emissions on ozone levels. In Belgium, the Netherlands, and Malta the contributions from anthropogenic emissions, and also from ship emissions, to annually averaged ozone are negative.

Contrary to what was shown for PM_{2.5} there are significant contributions from ROW shipping in most countries. For several countries in western and northern Europe, and in landlocked countries exemplified by Austria, as well as in Romania (partially bordering the Black Sea) (Figure 6), ROW shipping is the largest contributor to anthropogenic ozone levels both with regard to SOMO35 and annual average ozone, and the second largest in the Mediterranean countries where the by far largest

³SOMO35 is the indicator for health impacts recommended by WHO calculated as the daily maximum of 8-hour running ozone maximum over 35 ppb



contributions come from Mediterranean shipping. In and around the southern part of the North Sea
330 both land based and ship emissions of NO_x are high, and as also shown in Figure 5a,b,c,d, ozone
levels decrease as a result of North Sea and Baltic Sea shipping. In Belgium, the Netherlands, and
Malta the overall contributions of ship emissions from all sea areas give reductions in ozone levels.

3.3 Depositions of sulfur and oxidised nitrogen

Figure 2e,g shows the total (wet and dry) depositions of oxidised nitrogen and sulfur centred around
335 Europe. For oxidised nitrogen large depositions are calculated in north central Europe and in the Po
Valley in Italy. For sulfur the largest calculated depositions are mainly calculated in eastern Europe.

Figure 7 shows the contributions from the separate sea areas to depositions of oxidised nitrogen
and sulfur to selected countries. In addition, the source receptor relationships are listed in Tables 5
and 6 for both global and regional model calculations. Depositions from shipping are largely confined
340 to areas/countries near the sea, peaking close to major shipping routes, but sulfur depositions from
shipping are also low in and around the North Sea and Baltic Sea where sulfur emissions are very low
as a result of the SECA regulations.

4 Effects of CAP2020 on European $\text{PM}_{2.5}$ levels and on sulfur depositions

From January 1th 2020 the maximum allowed sulfur content in marine fuels was reduced to 0.5%
345 (CAP2020). Before CAP2020 the global average sulfur content outside SECAs was around 2.5%
although a higher percentage sulfur content of 3.5% was allowed. The latest figures showed that the
yearly average sulfur content of the residual fuel oils tested in 2017 was 2.54, see <http://www.imo.org/en/MediaCentre/HotTopics/GHG/Documents/2020%20sulphur%20limit%20FAQ%202019.pdf>. Our
calculations show that prior to CAP2020 the fraction of sulfate in $\text{PM}_{2.5}$ is low in the North Sea and
350 Baltic Sea, as well as in most of continental Europe and the British Isles as a result of the SECA
regulations. However, in sea areas outside the SECA, and in land areas bordering these sea areas,
sulfate is the major component in $\text{PM}_{2.5}$ origination from ship emissions (Figure 8a).

To give an estimate of the effects of CAP2020 on European $\text{PM}_{2.5}$ levels and the depositions of
oxidised sulfur we have made calculations reducing sulfur emissions outside the North Sea and the
355 Baltic Sea SECAs by 80%, corresponding to a reduction from 2.5% to 0.5% in the sulfur content
in the fuels. This is a crude estimate, as there are low emission ships operating outside the SECAs.
On the other hand CAP2020 compliance may not reach 100%. Furthermore we have assumed 80%
reductions in sulfur emissions also in low emissions zones far from European waters. But, as already
shown in Figure 3, emissions outside European waters (ROW shipping) has little or no effects on
360 European $\text{PM}_{2.5}$ levels. Figure 8b shows the calculated effects of CAP2020 on European $\text{PM}_{2.5}$
levels. Reductions in $\text{PM}_{2.5}$ ranging from 0.5 to more than $2\mu\text{gm}^{-3}$ are calculated in the major
shipping routes in the Mediterranean and eastern Atlantic ocean, affecting also neighbouring land



365 areas where ship emissions make up a significant percentage of the $PM_{2.5}$ concentrations. In European waters north of 62 degrees the sulphur fraction is also high, but here ship traffic is much lower and the effects on $PM_{2.5}$ well below $0.1\mu\text{gm}^{-3}$.

In Figure 4 the percentage anthropogenic contributions from all ships to selected European countries are shown calculated with ship emissions before and after CAP2020. In particular in the countries bordering the Mediterranean Sea, the percentage contributions to $PM_{2.5}$ relative to all anthropogenic emissions are reduced by about 50%. For countries bordering the North Sea and the Baltic Sea SECA, 370 where sulfur emissions prior to CAP2020 are very low, the percentage reductions in the contributions to $PM_{2.5}$ are much smaller.

A similar pattern as $PM_{2.5}$ is seen in Figure 7 for oxidised sulfur depositions, with substantial reductions in depositions of anthropogenic origin in countries bordering sea areas that are not NECAs as the Mediterranean Sea and the Northeast Atlantic.

375 5 Differences between regional and global model calculations

The regional model calculations as reported in the annual EMEP reports (exemplified by the latest EMEP report, EMEP Status Report 1/2019 (2019)) are widely used for regulative purposes within the EU and for the LRTAP convention (Convention on Long-Range Transboundary Air Pollution, url-<http://www.unece.org/fileadmin//DAM/env/lrtap/welcome.html>). The alternative global calculations 380 presented here gives an indication of the robustness of the officially reported calculations.

In general the results from the global and the regional model calculations are in good agreement. Even so there are some systematic differences in the model results. We have tried to trace these to differences listed below in model input and model setup, and to what extent global and regional calculations could give qualitatively and quantitatively different results for the effects of ship 385 emissions.

1. As discussed in section 2.1, Land based emissions are not identical.
2. The ship emission sets used in the global and regional calculations have a common origin (see section 2.1). Even so, annual emission totals for the individual sea areas differ. In the global calculations ship emissions in the individual sea areas are in general higher.
- 390 3. In the global model we reduce the emissions by 15% for all species in the sea areas simultaneously, whereas in the regional calculations emissions of the individual species are reduced separately.
4. The resolution used in the global and regional model calculations differ.
- 395 5. In the regional calculations the boundary and initial conditions for all gaseous and aerosol species were given as 5-year monthly average concentrations, derived from EMEP MSC-W global runs.



Bullet points 3 and 4 were a compromise to keep the computational demand of the global calculations within reasonable limits. Below we discuss the effects this makes for different components in detail. We also make statements on the processes behind these difference, which is of relevance also
400 beyond this study.

5.1 Differences in $PM_{2.5}$

For countries bordering the Baltic Sea and North Sea, the effects of ship emissions on $PM_{2.5}$ are consistently lower in the global versus the regional calculations (see Table 3). Most countries bordering the Baltic Sea and the North Sea are high emitters of ammonia. SO_4 (either emitted directly
405 or oxidised from SO_2) can react with ammonia forming ammonium sulfate. Much of the emitted NO_2 will form HNO_3 . Given ammonia in excess of SO_4 , HNO_3 will react with ammonia forming ammonium nitrate. As shown in Table 1 emissions of in particular sulfur in the European Union (and subsequently in countries bordering these two sea areas) are higher in the global model calculations, resulting in more ammonium sulfate formation and thereby allowing less of the HNO_3 from shipping
410 to form particulate ammonium nitrate. This explains the lower formation of $PM_{2.5}$ from shipping in the vicinity of regions of high ammonia emissions.

In several countries $PM_{2.5}$ levels from shipping are markedly higher in the global calculation, in particular in small countries such as Cyprus, and also in Portugal where the shipping lanes are very close to the shore. We believe this is caused by the lower resolution in the global calculations,
415 which implies that grid boxes covering partially land and sea extend further inland, thus artificially extending the effect of ship emissions somewhat further into these countries' territories.

5.2 Differences in nitrogen and sulfur deposition between global and regional model calculations

Above we argued that parts of the lower contributions from ships to $PM_{2.5}$ concentrations could
420 be caused by less ammonia available for ammonium nitrate formation in the global calculations, resulting in a higher HNO_3 to ammonium nitrate ratio. As the dry deposition of HNO_3 is faster than for ammonium nitrate, more oxidized nitrogen (mainly ammonium nitrate, HNO_3 , NO_2) is deposited in nearby countries where ammonia emissions are high.

In several countries both N and S depositions are higher, in particular in small countries such as
425 Malta and Cyprus, and in Portugal where the shipping lanes are very close to the shore. As for $PM_{2.5}$ concentrations, we believe this is caused by a lower resolution in the global calculations as grid boxes covering partially land and sea extend further inland.

5.3 Differences in SOMO35

In Table 4 the contributions from ship emissions to selected countries are listed, both for the global
430 and regional model calculations. Given the large compensating contributions from ozone titration,



mainly in winter, and ozone production, mainly in the summer months, SOMO35 calculated with the global and the regional model versions are remarkably similar. However, there are substantial differences, mainly confined to the very high NO_x emitting regions bordering the North Sea.

In the global calculations there are substantial contributions from ROW shipping that can not be attributed in the regional calculations. As shown in Table 4 there are substantial contributions from ROW, and in several countries ROW is the largest contributor.

With the ShipNOX parameterization included in the global calculations the contributions to SOMO35 from the sea areas is reduced by about 50% (see Figure 6) and considerably lower than in the regional calculations. ShipNOX is not used in the regional calculations, but the largest effects of ignoring the ship plume chemistry should be in low NO_x areas with large gradients between the plumes and ambient air most often found in pristine sea areas.

6 Conclusions

Emissions from shipping are large sources of air pollution and depositions of oxidised nitrogen and sulfur. In this study we have mainly restricted ourselves to the effects on European pollution levels, but the effects are global. In particular in coastal regions/countries, we attribute a large portion of the $\text{PM}_{2.5}$ of anthropogenic origin to emissions from shipping. For $\text{PM}_{2.5}$ we show that the largest contributions come from nearby waters. The calculations show that contributions from sulfur to $\text{PM}_{2.5}$ are low from the North Sea and the Baltic sea where the strict SECA regulations apply. Prior to the implementation of the CAP2020 regulations between 50% and 80% of the the anthropogenic $\text{PM}_{2.5}$ mass in countries/regions not bordering the SECAs was from sulfate. Here sulfate levels peak in summer when the conversion rate of SO_2 to sulphate is at its highest. In the SECA sea areas nitrates (mainly ammonium nitrate) is the largest constituent in anthropogenic $\text{PM}_{2.5}$, peaking in Spring as a result of the large ammonia emissions in nearby land areas in this season. With additional sulfate and gas phase HNO_3 from ship emissions, more ammonium (ammonium nitrate and ammonium sulphate) is formed, contributing about 20% - 30% of the $\text{PM}_{2.5}$ dry mass from shipping in much of the European land areas. As a result the combination of sulfur and NO_x emissions from shipping further increase the $\text{PM}_{2.5}$ burden in and around regions with high ammonia emissions beyond what strictly speaking is originating directly from SO_x and NO_x . Without ship emissions a larger portion of the ammonia would have been deposited to the surface and not contributing to the particle formation. The very low fraction of sulfate in $\text{PM}_{2.5}$ in and around the North Sea and the Baltic Sea demonstrates the effectiveness of the SECA regulations in reducing the $\text{PM}_{2.5}$ burden from shipping here. A global sulphur cap was implemented from January 1th 2020. This has resulted in substantial and immediate reductions in the $\text{PM}_{2.5}$ burden globally. This has resulted in approximately 50% reductions in $\text{PM}_{2.5}$ from shipping in European countries and regions not bordering the SECAs.



465 The net effects on surface ozone from ship emissions is a combination of ozone destruction, mainly
in winter, and ozone production, mainly in summer. This is also the reason for the different behaviour
of annual averaged ozone and the SOMO35 ozone metric. SOMO35 is hardly accumulated in winter
when ozone titration events are most frequent as ozone levels in winter are regularly below the 35ppb
threshold.

470 The lifetime of ozone in the atmosphere is considerably longer than for $PM_{2.5}$ ranging from hours
to a few days in the boundary layer to weeks and even months in the free troposphere (TF HTAP, 2010).
As a result ozone can be transported at intercontinental scales, explaining the large contributions from
ROW shipping.

Global model calculation require substantially more computer power than regional calculations,
475 and thus global scale source receptor calculations, even with a half a degree resolution, would not
be possible. The source receptor relationships derived from the global and regional calculations
are similar. Where there are differences, these can largely be attributed to model setup and input
data. Most of species levels, and the resulting surface depositions, highlighted in EMEP regional
calculations are relatively short-lived. As a result the effects of emissions originating outside the
480 regional model domain are small. Thus the additional benefits of global model calculations are small
compared to the potentially additional improvements in accuracy that can be achieved with higher
resolution in the regional calculations with higher resolution on a smaller model domain. For ozone
enhancing the resolution improves the representation of localised variations in NO_x to NMVOC
ratios explaining the differences in particular in the high NO_x countries bordering the North Sea. On
485 the other hand, with global scale calculations the contributions to ozone from all global sources can
be included. For several countries/regions we show that for ozone contributions from ROW shipping
are comparable, and in some regions higher, than contributions from sea areas bordering Europe.
In the regional model source receptor calculations bic (boundary and initial concentrations) only
account for ozone 'produced within the regional model domain from NO_x (emissions of NMVOC
490 from shipping are very small) transported from outside the regional model domain.

The dispersion and chemistry in the shipping plumes represents an uncertainty in the calculations.
Calculations including the "ShipNOX" parameterisation short circuit the NO_x chemistry so that only
50% of the emitted NO_x enters the ozone cycle, and as a result the effect of shipping on ozone is also
reduced by about 50%. Calculations with and without the "ShipNOX" parameterisation gives an upper
495 and lower range for the effects of shipping on ozone. The largest effects of ship plume chemistry are
likely to occur where the gradients between ship plume and ambient air NO_x concentrations are large.
Such conditions are less common in waters close to Europe.

Acknowledgements. This work has been partially funded by EMEP under UNECE. Computer time for EMEP
model runs was supported by the Research Council of Norway through the NOTUR project EMEP (NN2890K)
500 for CPU, and NorStore project European Monitoring and Evaluation Programme (NS9005K) for storage of data.



The National Center for Atmospheric Research is funded by the National Science foundation. The ship emission data have been downloaded from the ECCAD database <https://eccad.aeris-data.fr/>.



References

- Angelbratt, J., Mellqvist, J., Simpson, D., Jonson, J. E., Blumenstock, T., Borsdorff, T., Duchatelet, P., Forster, F., Hase, F., Mahieu, E., De Mazière, M., Notholt, J., Petersen, A. K., Raffalski, U., Servais, C., Sussmann, R., Warneke, T., and Vigouroux, C.: Carbon monoxide (CO) and ethane (C₂H₆) trends from ground-based solar FTIR measurements at six European stations, comparison and sensitivity analysis with the EMEP model, *Atmospheric Chemistry and Physics*, 11, 9253–9269, doi:10.5194/acp-11-9253-2011, <http://www.atmos-chem-phys.net/11/9253/2011/>, 2011.
- 505 Colette, A., granier, C., Hodnebrog, Ø., Jacobs, H., Maurizi, A., Nyíri, A., bessagnet, B., D'Angiola, A., D'Isidoro, M., Gauss, M., Meleux, F., Memmesheimer, M., Mieville, A., Rouïl, L., Russo, F., Solberg, S., Stordal, F., and Tampieri, F.: Air quality trends in Europe over the past decade: a first multi-model assessment, *Atmos. Chem. Phys.*, 11, 11 657–11 678, doi:10.5194/acp-11-11657-2011, <http://www.atmos-chem-phys.net/11/11657/2011/>, 2011.
- 510 Colette, A., Granier, C., Hodnebrog, Ø., Jakobs, H., Maurizi, A., Nyiri, A., Rao, S., Amann, M., Bessagnet, B., D'Angiola, A., Gauss, M., Heyes, C., Klimont, Z., Meleux, F., Memmesheimer, M., Mieville, A., Rouïl, L., Russo, F., Schucht, S., Simpson, D., Stordal, F., Tampieri, F., and Vrac, M.: Future air quality in Europe: a multi-model assessment of projected exposure to ozone, *Atmos. Chem. Phys.*, 12, 10 613–10 630, doi:10.5194/acp-12-10613-2012, <http://www.atmos-chem-phys.net/12/10613/2012/>, 2012.
- 515 Colette, A., Aas, W., Banin, L., Braban, C., Ferm, M., González Ortiz, A., Ilyin, I., Mar, K., Pandolfi, M., Putaud, J.-P., Shatalov, V., Solberg, S., Spindler, G., Tarasova, O., Vana, M., Adani, M., Almodovar, P., Berton, E., Bessagnet, B., Bohlin-Nizzetto, P., Boruvkova, J., Breivik, K., Briganti, G., Cappelletti, A., Cuvelier, K., Derwent, R., D'Isidoro, M., Fagerli, H., Funk, C., Garcia Vivanco, M., González Ortiz, A., Haeuber, R., Hueglin, C., Jenkins, S., Kerr, J., de Leeuw, F., Lynch, J., Manders, A., Mircea, M., Pay, M., Pritula, D., Putaud, J.-P., Querol, X., Raffort, V., Reiss, I., Roustan, Y., Sauvage, S., Scavo, K., Simpson, D., Smith, R., Tang, Y., Theobald, M., Tørseth, K., Tsyro, S., van Pul, A., Vidic, S., Wallasch, M., and Wind, P.: Air Pollution trends in the EMEP region between 1990 and 2012., *Tech. Rep. Joint Report of the EMEP Task Force on Measurements and Modelling (TFMM)*, Chemical Co-ordinating Centre (CCC), Meteorological Synthesizing Centre-East (MSC-E), Meteorological Synthesizing Centre-West (MSC-W) EMEP/CCC Report 1/2016, Norwegian Institute for Air Research, Kjeller, Norway, http://www.unece.org/fileadmin/DAM/env/documents/2016/AIR/Publications/Air_pollution_trends_in_the_EMEP_region.pdf, 2016.
- 520 Colette, A., Andersson, C., Manders, A., Mar, K., Mircea, M., Pay, M.-T., Raffort, V., Tsyro, S., Cuvelier, C., Adani, M., Bessagnet, B., Bergström, R., Briganti, G., Butler, T., Cappelletti, A., Couvidat, F., D'Isidoro, M., Doumbia, T., Fagerli, H., Granier, C., Heyes, C., Klimont, Z., Ojha, N., Otero, N., Schaap, M., Sindelarova, K., Stegehuis, A. I., Roustan, Y., Vautard, R., van Meijgaard, E., Vivanco, M. G., and Wind, P.: EURODELTA-Trends, a multi-model experiment of air quality hindcast in Europe over 1990–2010, *Geoscientific Model Development*, 10, 3255–3276, doi:10.5194/gmd-10-3255-2017, <https://www.geosci-model-dev.net/10/3255/2017/>, 2017.
- 535 Corbett, J., Winebrake, J., Green, E., Kasibhatla, P., and eyring A. laurer, V.: Mortality from ship emissions: A global assessment, *Environ. Sci. Tech.*, 4, 8512–8518, 2007.
- 540 Dore, A. J., Carslaw, D. C., Braban, C., Cain, M., Chemel, C., Conolly, C., Derwent, R. G., Griffiths, S. J., Hall, J., Hayman, G., Lawrence, S., Metcalfe, S. E., Redington, A., Simpson, D., Sutton, M. A., Sutton, P., Tang,



- Y. S., Vieno, M., Werner, M., and Whyatt, J. D.: Evaluation of the performance of different atmospheric chemical transport models and inter-comparison of nitrogen and sulphur deposition estimates for the UK, *Atmospheric Environment*, 119, 131–143, doi:10.1016/j.atmosenv.2015.08.008, 2015.
- 545 EMEP Status Report 1/2019: Transboundary particulate matter, photo-oxidants, acidifying and eutrophying components, EMEP MSC-W & CCC & CEIP, https://emep.int/publ/reports/2019/EMEP_Status_Report_1_2019.pdf, Norwegian Meteorological Institute (EMEP/MS-CW), Oslo, Norway, 2019.
- Endresen, Ø., Sørård, E., Sundet, J., Dalsøren, S., Isaksen, I., Berglen, T., and Gravir, G.: Emission from international sea transport and environmental impact, *J. Geophys. Res.*, 108, doi:10.1029/2002JD002898, 2003.
- 550 Eyring, V., Isaksen, I., Berntsen, T., Collins, W., Corbett, J., Endresen, Ø., Grainger, R., Moldanova, J., Schlager, H., and Stevenson, D.: Transport impacts on atmosphere and climate: Shipping, *Atmos. Environ.*, 44, 4735–4771, 2007.
- 555 Gaisbauer, S., Wankmüller, R., Matthews, B., Mareckova, K., Schindlbacher, S., Tista, M., and Ullrich, B.: Emissions for 2017, in: Transboundary particulate matter, photo-oxidants, acidifying and eutrophying components. EMEP Status Report 1/2019, pp. 43–64, The Norwegian Meteorological Institute, Oslo, Norway, 2019.
- Gauss, M., Tsyro, S., Fagerli, H., Hjellbrekke, A.-G., Aas, W., and Solberg, S.: EMEP MSC-W model performance for acidifying and eutrophying components, photo-oxidants and particulate matter in 2015., Supplementary material to EMEP Status Report 1/2017, available online at www.emep.int, The Norwegian Meteorological Institute, Oslo, Norway, 2017.
- 560 Gauss, M., Tsyro, S., Fagerli, H., Hjellbrekke, A.-G., Aas, W., and Solberg, S.: EMEP MSC-W model performance for acidifying and eutrophying components, photo-oxidants and particulate matter in 2016., Supplementary material to EMEP Status Report 1/2018, available online at www.emep.int, The Norwegian Meteorological Institute, Oslo, Norway, 2018.
- 565 Gauss, M., Tsyro, S., Benedictow, A., Fagerli, H., Hjellbrekke, A.-G., Aas, W., and Solberg, S.: EMEP MSC-W model performance for acidifying and eutrophying components, photo-oxidants and particulate matter in 2017., Supplementary material to EMEP Status Report 1/2019, available online at www.emep.int, The Norwegian Meteorological Institute, Oslo, Norway, 2019.
- 570 Huszar, P., Cariolle, D., Paoli, R., Halenka, T., Belda, M., Schlager, H., Miksovsky, J., and Pisoft, P.: Modeling the regional impact of ship emissions on NO_x and ozone levels over the Eastern Atlantic and Western Europe using ship plume parameterization, *Atmospheric Chemistry and Physics*, 10, 6645–6660, doi:10.5194/acp-10-6645-2010, <https://www.atmos-chem-phys.net/10/6645/2010/>, 2010.
- Höglund-Isaksson, L., Gómez-Sanabria, A., Klimont, Z., Rafaj, P., and Schöpp, W.: Technical potentials and costs for reducing global anthropogenic methane emissions in the 2050 timeframe –results from the GAINS model, *Environmental Research Communications*, 2, 025 004, doi:10.1088/2515-7620/ab7457, <https://doi.org/10.1088/2515-7620/ab7457>, 2020.
- IEA: World Energy Outlook 2018., Tech. rep., The Norwegian Meteorological Institute, Oslo, Norway, <https://www.iea.org/reports/world-energy-outlook-2018>, 2018.
- 580 Johansson, L., Jalkanen, J.-P., and Kukkonen, J.: Global assessment of shipping emissions in 2015 on a high spatial and temporal resolution, *Atmospheric Environment*, 167, 403 – 415,



- doi:<https://doi.org/10.1016/j.atmosenv.2017.08.042>, <http://www.sciencedirect.com/science/article/pii/S1352231017305563>, 2017.
- Johansson, L., Ytreberg, E., Jalkanen, J.-P., Fridell, E., Eriksson, K. M., Lagerström, M., Maljutenko, I., Raudsepp, U., Fischer, V., and Roth, E.: Model for leisure boat activities and emissions – implementation for the Baltic Sea, *Ocean Science Discussions*, 2020, 1–28, doi:10.5194/os-2020-5, <https://www.ocean-sci-discuss.net/os-2020-5/>, 2020.
- Jonson, J., Gauss, M., Schulz, M., and Nyíri, A.: Emissions from international shipping, in: *Transboundary particulate matter, photo-oxidants, acidifying and eutrophying components*. EMEP Status Report 1/2018, pp. 83–98, The Norwegian Meteorological Institute, Oslo, Norway, 2018a.
- Jonson, J. E., Schulz, M., Emmons, L., Flemming, J., Henze, D., Sudo, K., Tronstad Lund, M., Lin, M., Benedictow, A., Koffi, B., Dentener, F., Keating, T., Kivi, R., and Davila, Y.: The effects of intercontinental emission sources on European air pollution levels, *Atmospheric Chemistry and Physics*, 18, 13 655–13 672, doi:10.5194/acp-18-13655-2018, <https://www.atmos-chem-phys.net/18/13655/2018/>, 2018b.
- Karl, M., Jonson, J. E., Uppstu, A., Aulinger, A., Prank, M., Sofiev, M., Jalkanen, J.-P., Johansson, L., Quante, M., and Matthias, V.: Effects of ship emissions on air quality in the Baltic Sea region simulated with three different chemistry transport models, *Atmospheric Chemistry and Physics*, 19, 7019–7053, doi:10.5194/acp-19-7019-2019, <https://www.atmos-chem-phys.net/19/7019/2019/>, 2019.
- Liang, C.-K., West, J. J., Silva, R. A., Bian, H., Chin, M., Davila, Y., Dentener, F. J., Emmons, L., Flemming, J., Folberth, G., Henze, D., Im, U., Jonson, J. E., Keating, T. J., Kucsera, T., Lenzen, A., Lin, M., Lund, M. T., Pan, X., Park, R. J., Pierce, R. B., Sekiya, T., Sudo, K., and Takemura, T.: HTAP2 multi-model estimates of premature human mortality due to intercontinental transport of air pollution and emission sectors, *Atmospheric Chemistry and Physics*, 18, 10 497–10 520, doi:10.5194/acp-18-10497-2018, <https://www.atmos-chem-phys.net/18/10497/2018/>, 2018.
- Mills, G., Hayes, F., Simpson, D., Emberson, L., Norris, D., Harmens, H., and Büker, P.: Evidence of widespread effects of ozone on crops and (semi-)natural vegetation in Europe (1990–2006) in relation to AOT40- and flux-based risk maps, *Global Change Biology*, 17, 592–613, doi:10.1111/j.1365-2486.2010.02217.x, 2011a.
- Mills, G., Pleijel, H., Braun, S., Büker, P., Bermejo, V., Calvo, E., Danielsson, H., Emberson, L., Grünhage, L., Fernández, I. G., Harmens, H., Hayes, F., Karlsson, P.-E., and Simpson, D.: New stomatal flux-based critical levels for ozone effects on vegetation, *Atmos. Environ.*, 45, 5064 – 5068, doi:10.1016/j.atmosenv.2011.06.009, 2011b.
- Simpson, D., Benedictow, A., Berge, H., Bergström, R., Emberson, L., Fagerli, H., Flechard, C., Hayman, G., Gauss, M., Jonson, J., Jenkin, M., Nyíri, A., Richter, C., Semeena, V., Tsyro, S., Tuovinen, J.-P., Valdebenito, A., and Wind, P.: The EMEP MSC-W chemical transport model – technical description, *Atmos. Chem. Phys.*, 12, 7825–7865, doi:10.5194/acp-12-7825-2012, 2012.
- Simpson, D., Tsyro, S., and Wind, P.: Updates to the EMEP/MS-CW model, In *Transboundary particulate matter, photo-oxidants, acidifying and eutrophying components*. EMEP/MS-CW Status Report 1/2015, The Norwegian Meteorological Institute, Oslo, Norway, 2015.
- Simpson, D., Bergström, R., Tsyro, S., and Wind, P.: Updates to the EMEP MSC-W model, 2018 – 2019, EMEP Status Report 1/2019, available online at www.emep.int, The Norwegian Meteorological Institute, Oslo, Norway, 2019.



- Sofiev, M., Winebrake, J. J., Johansson, L., Carr, E. W., Prank, M., Soares, J., Vira, J., Kouznetsov, R., Jalkanen, J.-P., and Corbett, J. J.: Cleaner fuels for ships provide public health benefits with climate tradeoffs, *Nature*, 9, doi:10.1038/s41467-017-02774-9, 2018.
- 625 Stjern, C. W., Samset, B. H., Myhre, G., Bian, H., Chin, M., Davila, Y., Dentener, F., Emmons, L., Flemming, J., Haslerud, A. S., Henze, D., Jonson, J. E., Kucsera, T., Lund, M. T., Schulz, M., Sudo, K., Takemura, T., and Tilmes, S.: Global and regional radiative forcing from 20 % reductions in BC, OC and SO₄ – an HTAP2 multi-model study, *Atmospheric Chemistry and Physics*, 16, 13 579–13 599, doi:10.5194/acp-16-13579-2016, <http://www.atmos-chem-phys.net/16/13579/2016/>, 2016.
- 630 Tan, J., Fu, J. S., Dentener, F., Sun, J., Emmons, L., Tilmes, S., Sudo, K., Flemming, J., Jonson, J. E., Gravel, S., Bian, H., Davila, Y., Henze, D. K., Lund, M. T., Kucsera, T., Takemura, T., and Keating, T.: Multi-model study of HTAP II on sulfur and nitrogen deposition, *Atmospheric Chemistry and Physics*, 18, 6847–6866, doi:10.5194/acp-18-6847-2018, <https://www.atmos-chem-phys.net/18/6847/2018/>, 2018.
- TF HTAP: Hemispheric transport of air pollution. Part A: Ozone and particulate matter edited by: Frank Dentener, Terry Keating, and Hajime Akimoto, http://www.htap.org/publications/2010_report/2010_Final_Report/HTAP%202010%20Part%20A%20110407.pdf, 2010.
- 635 Theobald, M. R., Vivanco, M. G., Aas, W., Andersson, C., Ciarelli, G., Couvidat, F., Cuvelier, K., Manders, A., Mircea, M., Pay, M.-T., Tsyro, S., Adani, M., Bergström, R., Bessagnet, B., Briganti, G., Cappelletti, A., D’Isidoro, M., Fagerli, H., Mar, K., Otero, N., Raffort, V., Roustan, Y., Schaap, M., Wind, P., and Colette, A.: An evaluation of European nitrogen and sulfur wet deposition and their trends estimated by six chemistry transport models for the period 1990–2010, *Atmospheric Chemistry and Physics*, 19, 379–405, doi:10.5194/acp-19-379-2019, <https://www.atmos-chem-phys.net/19/379/2019/>, 2019.
- 640 Vinken, G. C. M., Boersma, K. F., Jacob, D. J., and Meijer, E. W.: Accounting for non-linear chemistry of ship plumes in the GEOS-Chem global chemistry transport model, *Atmospheric Chemistry and Physics*, 11, 11 707–11 722, doi:10.5194/acp-11-11707-2011, <https://www.atmos-chem-phys.net/11/11707/2011/>, 2011.
- Vivanco, M. G., Theobald, M. R., García-Gómez, H., Garrido, J. L., Prank, M., Aas, W., Adani, M., Alyuz, U., Andersson, C., Bellasio, R., Bessagnet, B., Bianconi, R., Bieser, J., Brandt, J., Briganti, G., Cappelletti, A., Curci, G., Christensen, J. H., Colette, A., Couvidat, F., Cuvelier, C., D’Isidoro, M., Flemming, J., Fraser, A., Geels, C., Hansen, K. M., Hogrefe, C., Im, U., Jorba, O., Kitwiroon, N., Manders, A., Mircea, M., Otero, N., Pay, M.-T., Pozzoli, L., Solazzo, E., Tsyro, S., Unal, A., Wind, P., and Galmarini, S.: Modeled deposition of nitrogen and sulfur in Europe estimated by 14 air quality model systems: evaluation, effects of changes in emissions and implications for habitat protection, *Atmospheric Chemistry and Physics*, 18, 10 199–10 218, doi:10.5194/acp-18-10199-2018, <https://www.atmos-chem-phys.net/18/10199/2018/>, 2018.
- 650



Table 1. Ship emissions from FMI in European sub sea areas. Sulphur emissions are given as SO₂. PM emissions are sub-divided into Ash, EC and OC, all assumed emitted as PM_{2.5}. Total EU emissions used in global and regional calculations are also listed. 5% of these SO₂ are assumed to be emitted as SO₄.

	Sulphur		NOx	CO	PM_{2.5}			NMVOC
	Gg SO ₂		Gg NO ₂	Gg CO	see caption			Gg as C
	SO ₂	SO ₄			Ash	EC	OC	
Global	9408	559	19670	1360	91	124	309	150
Mediterranean Sea	680	40	1340	92	6.4	8.7	22	11
Black Sea	66	3.8	158	12	0.8	1.1	2.7	1.3
Baltic Sea	9.9	0.7	313	21	1.5	2.0	4.9	2.6
North Sea	27	1.6	684	52	3.4	4.6	11.8	5.8
Remaining Atl.	456	27	836	60	4.0	5.4	13.5	6.5
European Union emissions								
EU Global 2017	2621		7723	18227	1490			6245
EU EMEP 2017	2274		7537	25737	1303			7014



Table 2. Overview of model scenarios used. Separate model spin-up was only performed for base model run(s) and for model runs with globally perturbed emissions. For SR model runs perturbing limited areas we use the same spin-up as for the Base runs. CAP2020 emissions are estimated by scaling the emissions outside the North Sea and Baltic Sea SECAs from an assumed pre-CAP2020 global average sulfur content of 2.5% to 0.5%. Additional information about the model scenarios is given in section 2.2.

Scenario	Description	spin-up
Scenarios without ShipNOX		
Base_2017	2017 emissions unperturbed	5 months
SR_AllAnt	All anthropogenic emissions reduced 15%	5 months
SR_AllSh	All ship emissions reduced 15%	5 months
SR_BALNOS	North Sea and Baltic Sea emissions reduced 15%	as Base_2017
SR_MEDBLS	Mediterranean and Black Sea emissions reduced 15%	as Base_2017
SR_ATL	Remaining NE Atlantic emissions reduced by 15% S	as Base_2017
SR_ROW	Rest Of World ship emissions reduced 15%	5 months
Scenarios with CAP2020		
CAP2020_Base	2017 emissions unperturbed	5 months
CAP2020_SR_AllAnt	All anthropogenic emissions reduced 15%	5 months
CAP2020_SR_AllSh	All ship emissions reduced 15%	5 months
Scenarios with ShipNOX		
SHN_Base_2017	2017 emissions unperturbed	5 months
SHN_SR_AllAnt	All anthropogenic emissions reduced 15%	5 months
SHN_SR_AllSh	All ship emissions reduced 15%	5 months
SHN_SR_BALNOS	North Sea and Baltic Sea emissions reduced 15%	as SHN_Base_2017
SHN_SR_MEDBLS	Mediterranean and Black Sea emissions reduced 15%	as SHN_Base_2017
SHN_SR_ATL	Remaining NE Atlantic emissions reduced by 15% S	as SHN_Base_2017
SHN_SR_ROW	Rest Of World ship emissions reduced 15%	5 months



Table 3. Source receptor relationships for PM_{2.5} from shipping. GL17 and GL20 calculated by the global model with 2017 and CAP2020 ship emissions respectively. The scenario calculations are made reducing the ship emissions for all species by 15%. “EMEP” is the source receptor calculations for 2017 from the latest EMEP report (EMEP Status Report 1/2019, 2019) appendix B. The EMEP source receptor reporting are based on separate calculations of individual species from all European countries and sea areas. **Glob** is the contribution from all global shipping, **NOS + BAS** from the North Sea and Baltic Sea combined, **MED + BLS** the Mediterranean Sea and Black Sea combined and **ATL** is the North Atlantic. ROW includes all ship emissions outside the individual sea areas listed. For the “EMEP” reporting boundary and initial contributions are listed. Units: ng/m³ per 15% emission reduction.

Country	Glob		NOS + BAS		MED + BLS		ATL		ROW
	GL17	GL20	GL17	EMEP	GL17	EMEP	GL17	EMEP	GL17
Countries bordering the Baltic Sea									
Estonia	22	21	20	22	0	0	2	1	1
Latvia	22	21	19	22	0	0	2	2	1
Lithuania	26	25	22	26	1	1	2	1	1
Finland	8	7	5	7	0	0	2	2	0
Denmark	110	107	99	112	1	0	8	6	3
Sweden	16	14	13	15	0	0	3	3	0
Poland	30	28	22	22	2	2	3	3	4
Countries bordering the North Sea									
Belgium	108	99	74	82	4	3	21	20	11
Germany	69	64	51	52	3	2	8	5	6
Netherlands	163	154	128	140	3	2	22	22	11
Norway	8	4	2	5	0	0	5	4	0
GB	68	52	28	34	1	1	35	33	3
Countries bordering the North Atlantic									
Ireland	42	29	12	11	0	0	28	28	2
Portugal	92	38	1	1	19	8	70	34	2
Iceland	5	2	1	1	0	0	4	3	0
Countries bordering the Mediterranean and Black Sea									
Spain	92	42	2	2	63	57	25	23	2
France	77	54	29	31	20	17	24	23	4
Greece	90	36	1	0	87	73	1	1	2
Malta	330	126	1	1	324	347	2	2	2
Italy	136	78	3	2	126	102	3	2	4
Cyprus	177	75	0	0	173	120	1	0	2
Bulgaria	21	11	1	1	18	21	1	1	1
Romania	17	11	3	3	11	12	2	1	1



Table 4. Source receptor relationships for SOMO35 from shipping as calculated by the global model, GL17, without SHIPNOX, see section 2, and as reported in EMEP Status Report 1/2019 (2019) appendix B. All the calculations are made with 2017 emissions and meteorological data. **Glob** is the contribution from all global shipping, **NOS + BAS** from the North Sea and Baltic Sea combined, **MED + BLS** the Mediterranean Sea and Black Sea combined and **ATL** is the North Atlantic. ROW includes the effects from all ship emissions outside the above listed individual sea areas. BIC is regional Boundary and Initial Concentrations. Units: ppb.days per 15% emission reduction.

Country	Glob		NOS + BAS		MED + BLS		ATL		ROW	
	GL17	BIC	GL17	EMEP	GL17	EMEP	GL17	EMEP	GL17	BIC
Countries bordering the Baltic Sea										
Estonia	20		8	10	1	0	4	3	8	13
Latvia	22		9	10	1	0	4	3	8	14
Lithuania	22		8	9	1	1	5	4	8	15
Finland	15		3	4	1	0	3	3	7	10
Denmark	10		-9	-3	1	0	8	7	10	20
Sweden	18		3	6	1	0	5	4	9	14
Poland	19		5	5	1	1	5	4	8	18
Countries bordering the North Sea										
Belgium	1		-15	-10	1	1	6	7	8	20
Germany	14		-33	-2	1	1	6	6	9	21
Netherlands	-12		-26	-18	1	0	6	6	7	18
Norway	23		4	5	1	0	7	5	12	17
GB	16		-5	-2	1	0	7	8	12	19
Countries bordering the North Atlantic										
Ireland	24		-1	0	1	0	9	10	14	19
Portugal	47		1	0	3	5	25	28	17	41
Iceland	29		3	3	1	0	9	6	16	19
Countries bordering the Mediterranean and Black Sea										
Spain	37		1	0	7	13	13	14	16	39
France	26		-0	0	5	7	10	10	12	25
Italy	43		3	1	24	33	5	4	10	25
Greece	46		3	2	30	35	3	2	10	26
Malta	53		3	1	31	22	6	4	13	25
Cyprus	115		2	0	100	75	2	1	11	27
Bulgaria	25		3	2	9	10	3	2	10	24
Romania	22		4	2	5	6	3	2	9	22
Landlocked countries										
Austria	24		3	2	4	5	5	4	11	23
Switzerland	26		2	1	4	6	6	5	13	26
Czechia	21		3	2	2	2	6	5	10	22



Table 5. Source receptor relationships for depositions of Dep of ox.N from shipping as calculated by the global model and as reported for year 2017. **Glob** is the contribution from all global shipping, **NOS + BAS** from the North Sea and Baltic Sea combined, **MED + BLS** the Mediterranean Sea and Black Sea combined and **ATL** is the North Atlantic. GL17 are from the global model calculations, end EMEP 2014 are from EMEP Status Report 1/2019 (2019) appendix B. Units: 100 Mg of N/S per 15% emission reduction.

Country	Glob		NOS + BAS		MED + BLS		ATL		ROW	
	GL17		GL17	EMEP	GL17	EMEP	GL17	EMEP	GL17	BIC
Countries bordering the Baltic Sea										
Estonia	123		27	26	0	0	4	1	1	0
Latvia	39		36	34	1	1	2	1	1	1
Lithuania	37		34	30	1	1	2	1	1	1
Finland	99		88	84	1	1	8	6	1	10
Denmark	55		51	45	0	0	3	3	1	2
Sweden	201		183	163	1	1	15	13	2	16
Poland	166		143	126	7	6	10	8	6	11
Countries bordering the North Sea										
Belgium	38		31	25	1	1	5	4	2	4
Germany	286		238	197	9	8	27	23	13	29
Netherlands	72		62	48	1	1	7	6	2	6
Norway	116		88	86	1	1	26	22	2	22
GB	161		88	78	2	2	66	58	7	28
Countries bordering the North Atlantic										
Ireland	22		6	5	1	0	14	13	2	9
Portugal	51		1	1	9	8	39	34	2	10
Iceland	8		3	2	0	0	4	6	1	12
Countries bordering the Mediterranean and Black Sea										
Spain	232		6	5	144	116	77	67	6	46
France	306		124	110	81	74	90	80	11	43
Italy	227		9	6	207	176	7	6	3	22
Greece	89		2	1	84	70	1	1	1	9
Bulgaria	32		4	3	27	23	1	1	1	5
Romania	46		13	10	28	25	2	1	1	8
Landlocked countries										
Austria	23		12	9	7	6	2	2	1	3
Switzerland	11		5	4	4	4	2	1	1	2
Czech Rep	29		22	17	3	2	2	2	2	3



Table 6. Source receptor relationships for depositions of Dep of ox.S from shipping as calculated by the global model and as reported for year 2017. **Glob** is the contribution from all global shipping, **NOS + BAS** from the North Sea and Baltic Sea combined, **MED + BLS** the Mediterranean Sea and Black Sea combined and **ATL** is the North Atlantic. GL15 is from the global model calculations, 2014 is from ? and 2016 from Appendix ?? in this report. Units: ppb.days per 15% emission reduction.

Country	Glob		NOS + BAS		MED + BLS		ATL		ROW	
	GL17	GL20	GL17	EMEP	GL17	EMEP	GL17	EMEP	GL17	BIC
Countries bordering the Baltic Sea										
Estonia	2	1	1	1	0	0	0	0	0	3
Latvia	3	2	1	1	1	1	1	0	0	6
Lithuania	2	1	1	1	1	1	1	1	0	6
Finland	8	4	3	3	1	1	3	2	0	21
Denmark	5	4	3	2	0	0	2	1	0	6
Sweden	16	10	8	7	1	1	6	5	0	33
Poland	10	3	2	2	4	4	4	4	0	13
Countries bordering the North Sea										
Belgium	6	4	3	2	0	0	2	2	0	4
Germany	39	23	19	9	6	6	12	10	1	50
Netherlands	15	12	12	5	0	0	3	2	0	5
Norway	25	9	5	6	1	0	19	15	0	45
GB	54	15	6	5	2	2	46	36	1	41
Countries bordering the North Atlantic										
Ireland	12	3	0	1	1	0	14	13	2	9
Portugal	31	6	0	0	5	4	25	20	1	13
Iceland	8	1	0	0	0	0	3	3	0	22
Countries bordering the Mediterranean Sea										
Spain	154	32	0	0	101	68	52	40	1	63
France	119	30	8	8	57	47	52	43	1	75
Italy	145	29	0	0	139	105	5	3	1	39
Greece	62	13	0	0	61	43	1	0	0	16
Bulgaria	17	3	0	0	16	13	1	0	0	16
Romania	21	4	0	0	19	16	1	1	0	23
Landlocked countries										
Austria	6	2	1	0	5	4	1	1	0	11
Switzerland	4	1	0	0	3	3	1	1	0	7
Czech Rep	3	1	0	0	2	2	1	1	0	10

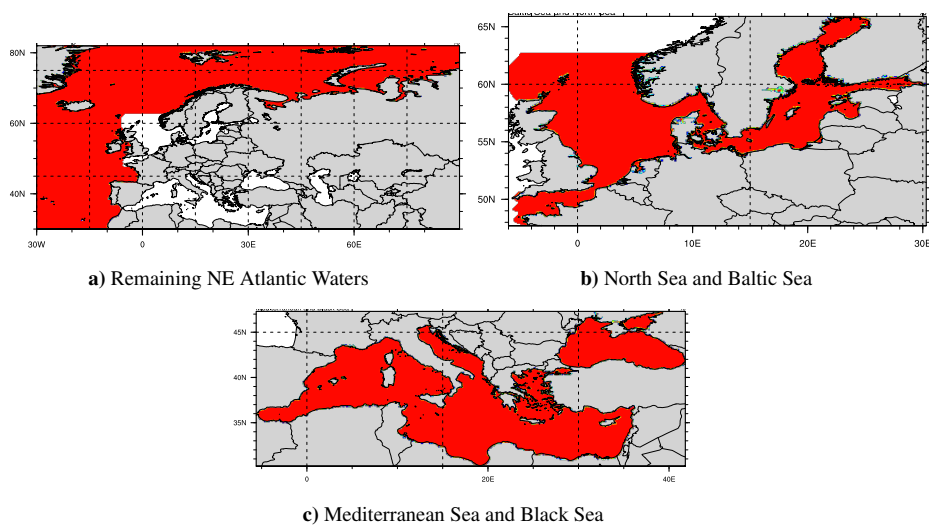


Figure 1. The individual sea areas marked in red. Shipping emissions in all other sea areas classified as ROW (Rest Of World) shipping.

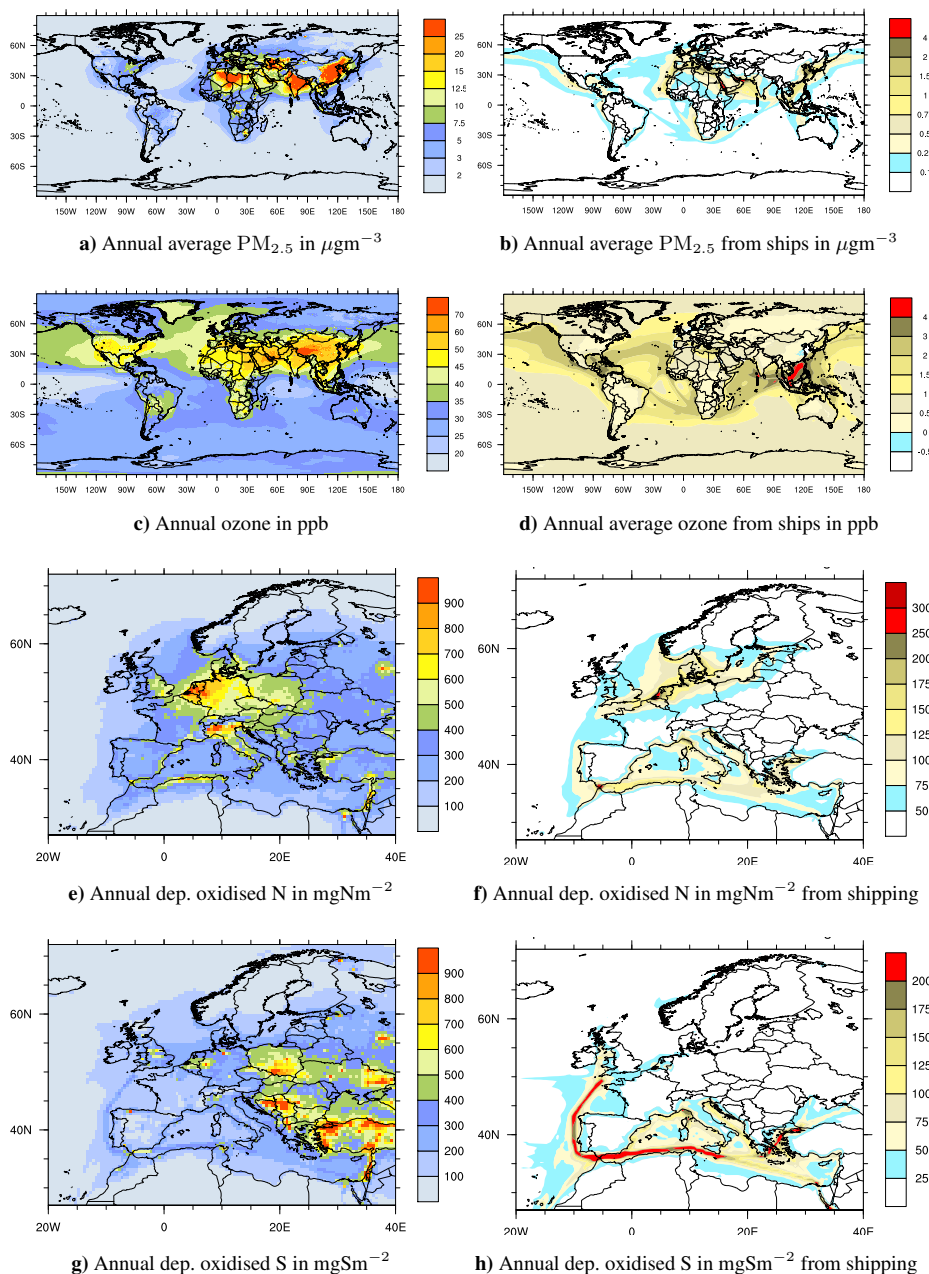


Figure 2. Right: Annually averaged global concentrations of $PM_{2.5}$ a) and O_3 c). Depositions of oxidised nitrogen e) and sulfur g). Left: Contributions from global shipping to $PM_{2.5}$ b) and O_3 d) and to depositions of oxidised nitrogen f) and sulfur h).

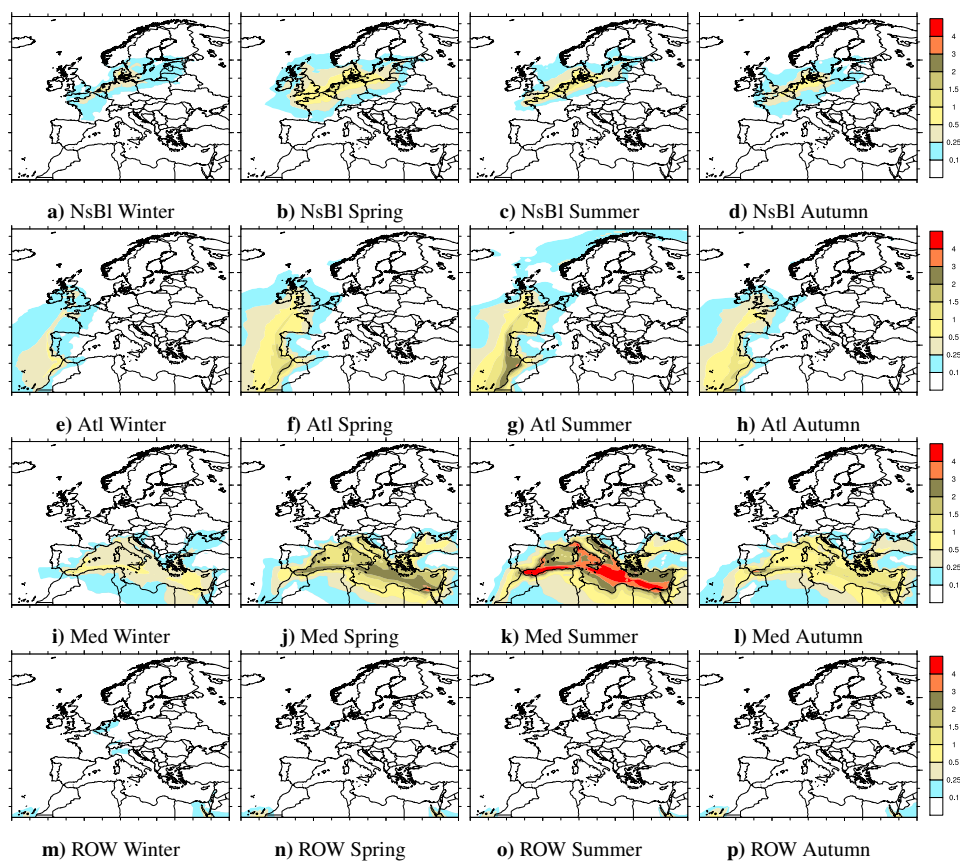


Figure 3. Seasonal contributions to European $\text{PM}_{2.5}$ levels (in $\mu\text{g m}^{-3}$) from 15% perturbations of the emissions in separate sea areas defined in section 2.2. The perturbations are multiplied by 100/15. Winter defined as December–January, Spring: March–May, Summer: June–August, Autumn: September–November.

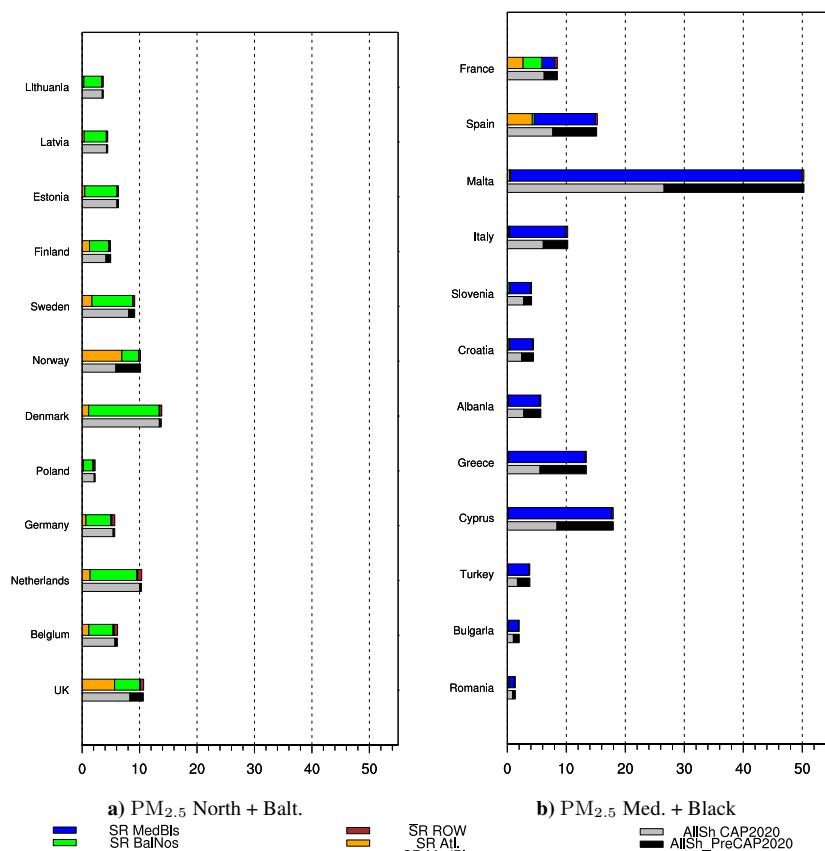


Figure 4. Percentage contributions from shipping to annually averaged PM_{2.5} to countries bordering the North Sea and the Baltic Sea (left) and the Mediterranean Sea and the Black Sea (right) relative to contributions from all global anthropogenic emissions. Contributions are shown both for all ships and separated by sea area. For each country the contributions from the individual sea areas are added in the upper bar and the contributions from all ship emissions calculated as the difference between the Base and SR_AllShips scenarios are shown as black + grey bar below. The Base - SR_AllShips bars are split in a black and grey part where the first grey part represents the contributions after CAP2020 and black + grey the contributions prior to CAP2020. Differences in length between All ships (Black + grey) and the added contributions from the separate sea areas is an indication of non-linear effects.

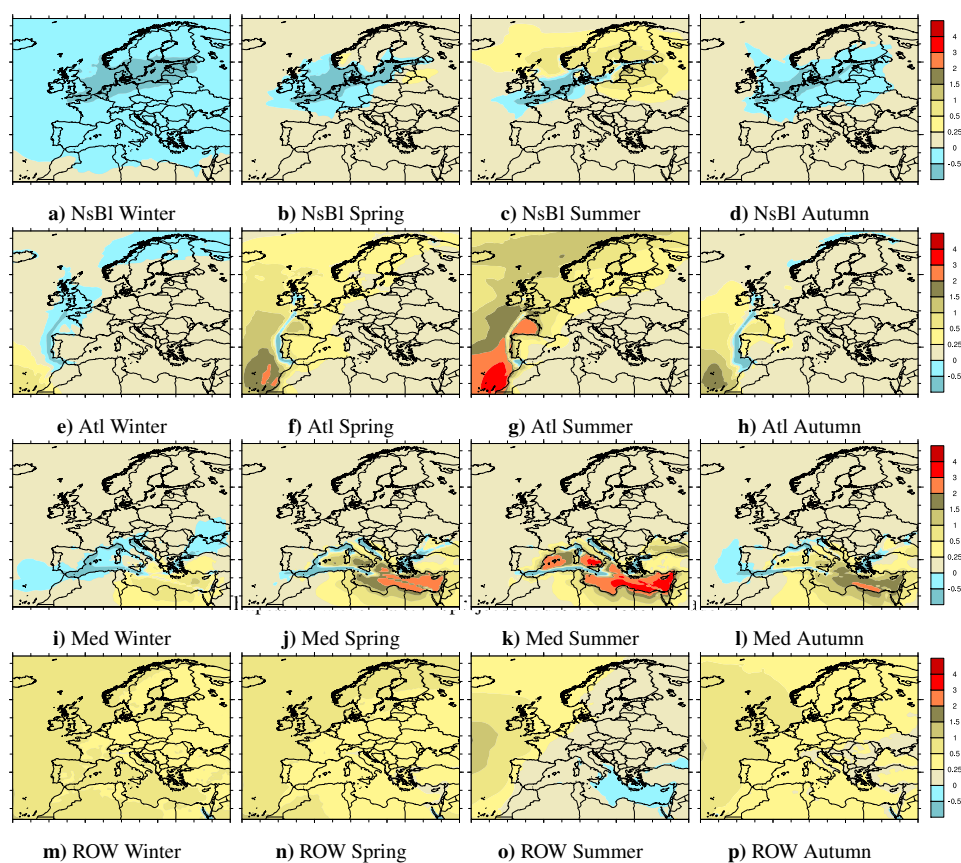


Figure 5. Seasonal contributions to European ozone levels (in ppb) from 15% perturbations of the emissions in separate sea areas defined in section 2.2. The perturbations are multiplied by 100/15. Winter defined as December–January, Spring: March–May, Summer: June–August, Autumn: September–November.

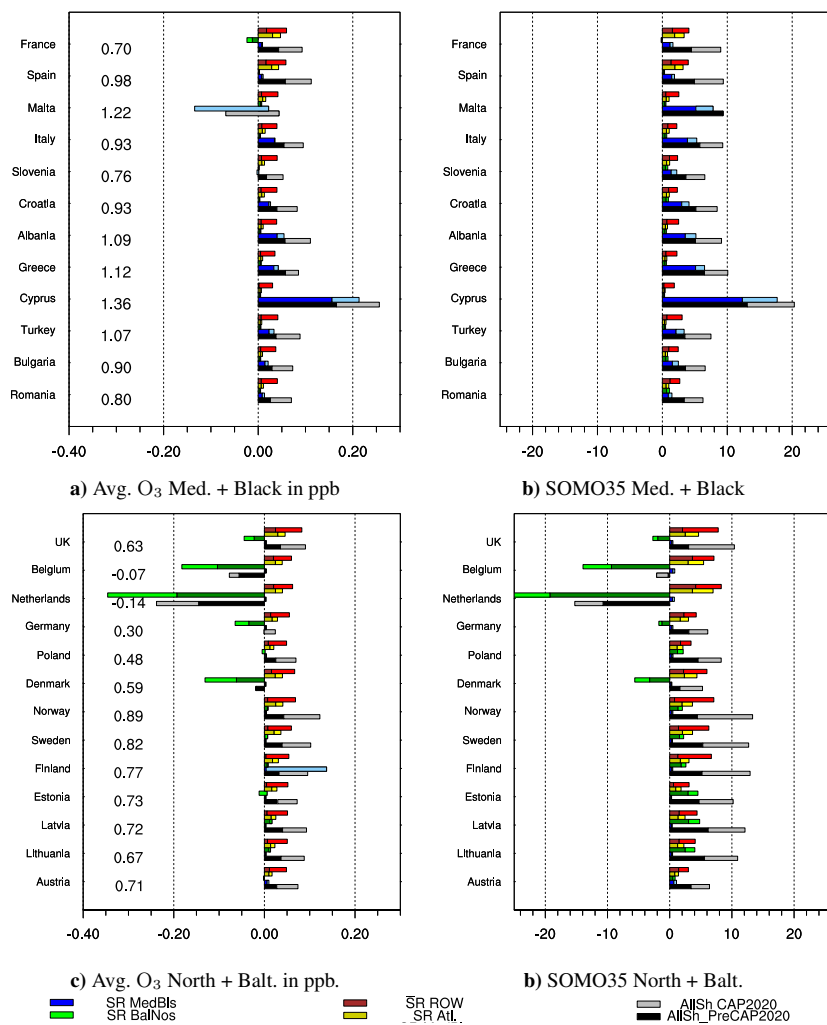


Figure 6. Contributions from shipping in ppb to annually averaged ozone from 15% reductions in ship emissions (left). Numbers to the right of the country names are the effects of the 15% reductions of all anthropogenic emissions calculated as Base_2017 – SR_AllSh. Right, percentage contributions to SOMO35 relative to contributions from all global anthropogenic emissions. Contributions are shown for all ships and separated by sea area. The length of the bars are split so that the darker parts of the bars represent calculations assuming SHIPNOX (see section 2) and the full length without SHIPNOX. Note that for Malta the smaller perturbation in NO_x from Mediterranean shipping with SHIPNOX results in a small ppb increase in calculated ozone, whereas the larger perturbation without SHIPNOX results in a decrease.

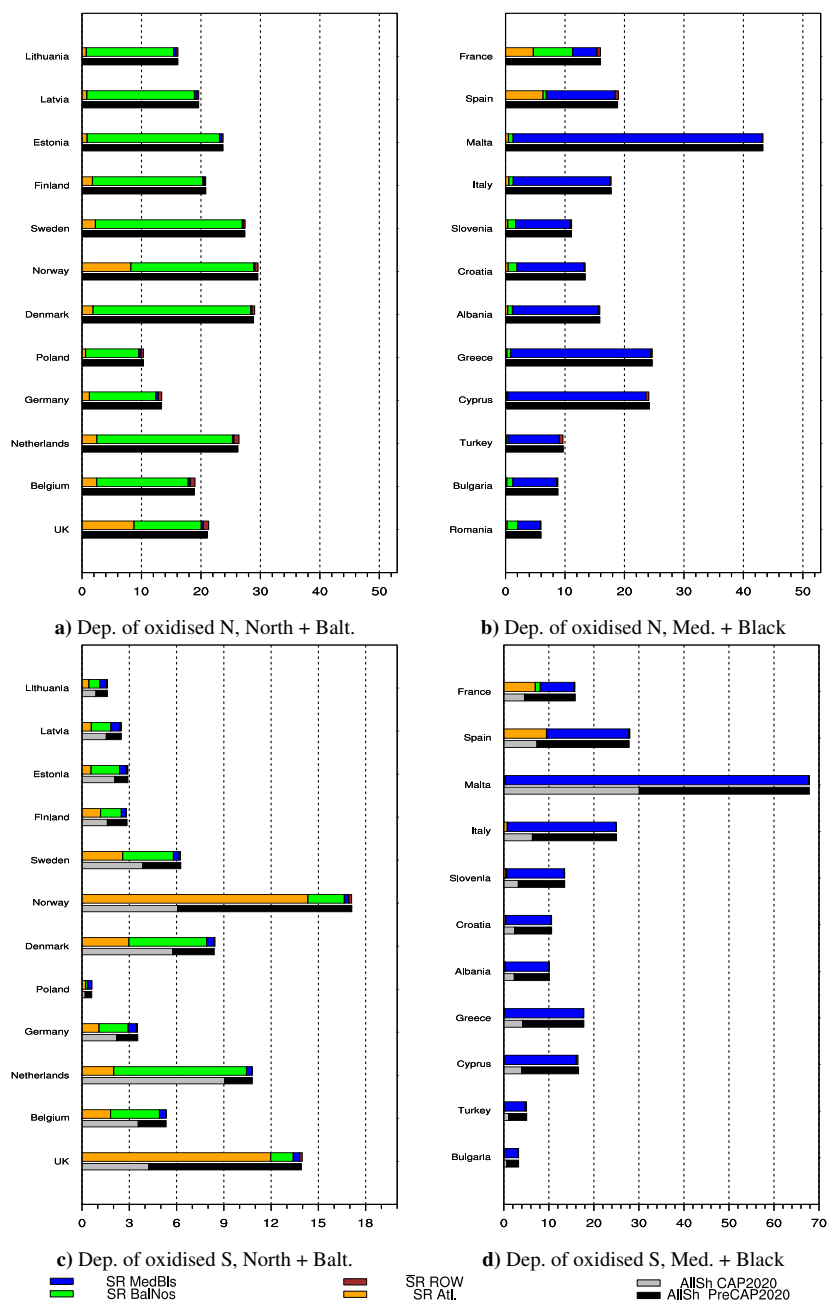


Figure 7. Percentage contributions from shipping to annually averaged depositions of oxidised nitrogen (top) and sulfur (bottom) relative to contributions from all global anthropogenic emissions. Contributions are shown for all ships and separated by sea area. see also caption in Figure 4.

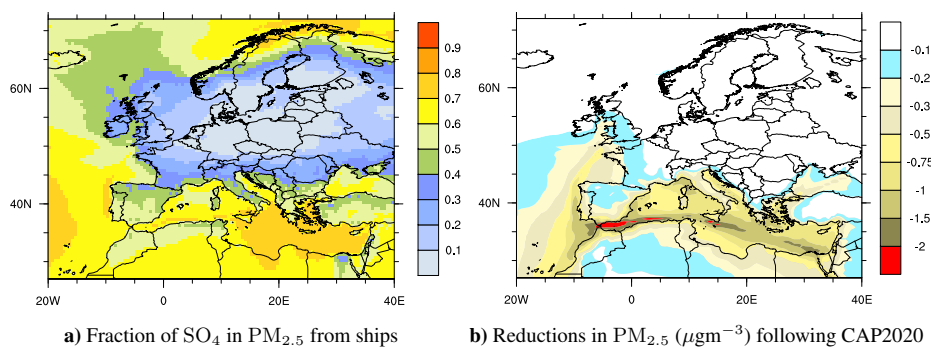


Figure 8. Fraction of SO₄ in PM_{2.5} in European waters from shipping a). Reductions in PM_{2.5} (μg m⁻³) following the CAP2020 regulations.